Resonance Effect on Self- and Inter-Association Hydrogen Bonding Interaction of Polymer Blend

Chien-Ting Lin,[†] Shiao-Wei Kuo,*[,‡] Jen-Chih Lo,[†] and Feng-Chih Chang*[,†]

Institute of Applied Chemistry, National Chiao Tung University, Hsin Chu 300, Taiwan, and Department of Materials and Optoelectronic Science, Center for Nanoscience and Nanotechnology, National Sun Yat-Sen University, Kaohsiung 804, Taiwan

Received: November 14, 2009; Revised Manuscript Received: December 14, 2009

A comparative study of three poly(methacrylamides) containing different N-substitutions was carried out in order to obtain a better understanding of the resonance effects on the inter-association and self-association hydrogen bonding interactions in polymer blends. DSC and solid-state NMR analyses are employed to study the relative miscibility of these three binary blends, indicating that the PNPAA/P4VP blend has a better miscibility than the PNMAA/P4VP and PNCHAA/P4VP blends, because the resonance characteristic of the aromatic ring in PNPAA enhances the inter-association hydrogen bonding with P4VP based on FTIR and solid-state NMR analyses.

Introduction

Specific interactions between various polymers containing different structures have been intensively reported, especially for those in hydrogen bonding blend systems such as homopolymer/homopolymer,[1−4] homopolymer/copolymer,[5−11] ternary blends,[12−14] and polymer nanocomposites.[15,16] Most studies have concentrated on the understanding of structural effects on self- and inter-associative hydrogen bonding in polymer blends. The accessibility of functional groups in hydrogen-bonded polymer blends can significantly affect the intramolecular screening effects which are a direct consequence of chain connectivity.[17−19] Moreover, the presence of bulky side groups can also reduce the accessibility of the functional groups as functional group accessibility effects. Painter et al. studied the 2,3-dimethylbutadiene-*stat*-4-vinylphenol (DMBVPh) blending with a homogeneous series of poly(*n*-alkyl methacrylates) (PAMA) and showed that the accessibility of the PAMA carbonyl groups decreases as the length of the PAMA side chains is increased.[19] In our previous study on poly(methyl methacrylate-*co*-methacrylamide-*co*-styrene) (PMMA-*co*-PMAAM-*co*-PS) terpolymers, the inter-associative hydrogen bonding between the amide group of PMAAM and the carbonyl group of PMMA is increased upon the addition of PS units because these PS units play an inert diluent role on the PMAAM polymer chain and thus reduce the strength of its self-associative hydrogen bonding.[20−22] In addition, the acidity or basicity of the hydrogen bond donor, steric hindrance, and temperature can also affect the inter-association hydrogen bonding in polymer blend systems.[2,23]

The steric bulky aromatic side group can play as an inert diluent and also possess resonance characteristics. Comparing aliphatic methylamine and cyclohexylamine with aromatic aniline, the pK_b values of aniline show a significantly weaker base than methylamine and cyclohexylamine, as shown in Table 1.[24] This reduced basicity of aniline is due to resonance delocalization of the lone-paired electrons on the nitrogen atom.

TABLE 1: Values of pK_b for Methylamine, Aniline, and Cyclohexylamine

amine	K_b	pK_b[a]
methylamine	4.3×10^{-4}	3.36[a]
aniline	4.0×10^{-9}	9.40
cyclohexylamine	4.7×10^{-4}	3.33

[a] Stronger bases have smaller values of pK_b.

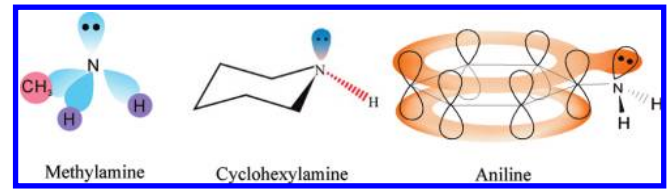

Figure 1. Chemical structures of methylamine, aniline, and cyclohexylamine.

Figure 1 shows that the lone-paired electrons on the nitrogen atom of the aniline are delocalized over the π system of the ring. This overlap is impossible in the anilinium ion, so that reactant (aniline) is stabilized in comparison to the product. The basicity of lone-paired electrons on nitrogen is affected by the resonance effect, and the N−H bonding in the amide unit is also affected by the resonance. In small molecules, the resonance-assisted effect on self-associative hydrogen bonding can be analyzed by the atoms in molecules (AIM) theory and density functional theory (DFT).[25,26] The donor−acceptor distance of the *cis*-enol tautomer of the malonaldehyde is reduced by the π-electron delocalization between the donor and acceptor atoms to enhance the strength of malonaldehyde's intramolecular hydrogen bonding.[25] These theories may be difficult to apply in polymers because the chain connectivity complicates hydrogen bonding in the polymer system, but the resonance effect cannot be ignored.

In methane, CH_4, there are four hybridized orbitals, sp^3, and each sp^3 orbital is occupied by four C−H bonds. The ideal shape represented by sp^3 hybridization is a tetrahedron, causing each bond angle to be 109.5°.[24] In ethene, $CH_2{=}CH_2$, one s orbital and two p orbitals of a carbon atom are hybridized to three sp^2

* To whom all correspondence should be addressed. E-mail: kuosw@faculty.nsysu.edu.tw. Fax: 886-7-5254099. E-mail: changfc@mail.nctu.edu.tw. Fax: 886-3-5131512.
[†] National Chiao Tung University.
[‡] National Sun Yat-Sen University.

10.1021/jp910849y
Published on Web 01/07/2010

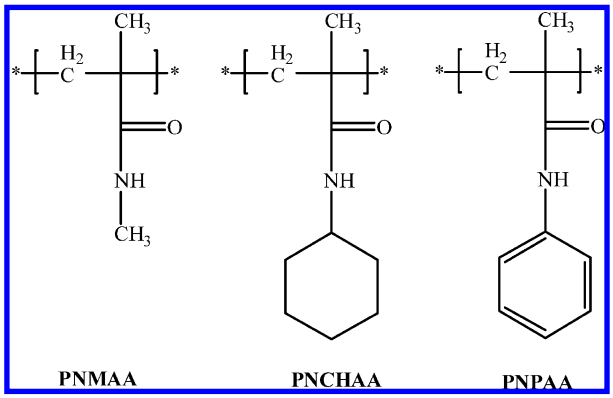

Figure 2. Chemical structures of poly(*N*-methyl methacrylamide) (PNMAA), poly(*N*-cyclohexyl methacrylamide) (PNCHAA), and poly(*N*-phenyl methacrylamide) (PNPAA).

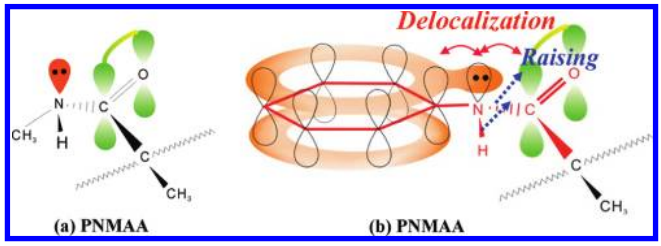

Figure 3. N-Substitution of (a) PNMAA and (b) PNPAA, affecting the lone pair electrons on the nitrogen atom and the π bonding electrons of the carbonyl group.

orbitals. Therefore, the axes of these three orbitals lie in a plane directed toward the corners of an equilateral triangle with the carbon nucleus at the center, implying that these three bond angles between three sp^2 orbitals are 120°. The unhybridized p orbital is perpendicular to the plane defined by the axes of the sp^2 orbitals. Figure 2 shows the chemical structures of three poly(methacrylamides) used in this study. The lone-paired electrons on the nitrogen atom occupy one of the sp^3 tetrahedral positions. In poly(*N*-phenyl methacrylamide), as shown in Figure 3, the lone-paired electrons on nitrogen delocalize over the π system of the aromatic ring and carbonyl group simultaneously, to reach a more stable state. The originally ideal tetrahedral is distorted, expanding the C—N—H or C—N—C bond angles while compressing the angle between lone pair and N—H bonding to form a near plane arranged by the phenyl group, nitrogen atom, and carbonyl group. The geometry is similar to a combination of sp^2 hybridization with one p orbital as ethene. As a result, the N—H bonding occupies one of the sp^2 hybridization positions, and the lone pair electrons occupy the p orbital to delocalize over the π system of the aromatic ring and carbonyl group. Therefore, compared with poly(*N*-methylmethacrylamide), the electron-cloud distribution of the (O═)C—N—H group in poly(*N*-phenyl methacrylamide) is near a planar, and the self- and inter-association behaviors of the amide group in poly(*N*-phenyl methacrylamide) are not expected to be the same as in poly(*N*-methyl methacrylamide).

In a polymer blend with inter-association hydrogen bonding, competitive self-association exists between polymer chains of hydrogen-bond donors (i.e., phenol, amide, and acid). The competition of self- and inter-association hydrogen bonding in polymer blends affects the miscibility of polymer blends, and numerous investigations have been reported during recent years.[27,28] Some of these reports aim at the phase separation caused by the difference in the interaction energy of the binary or ternary system.[29,30] Liu et al.[27] reported that the strong hydrogen-bonded self-association of the vinyl phenol segment in poly(styrene-*co*-4-vinyl phenol)/poly(styrene-*co*-4-vinyl pridine) (STVPh/STVPy) blends dominates over the immiscibility-to-miscibility transition in controlling the surface composition. Extent of self- and inter-association hydrogen-bonded phenol controlled by the vinyl phenol content in STVPh, a controllable surface enrichment of polymer blends can be obtained. In our previous works about polymer blends of poly(vinyl phenol) (PVPh) and poly(acetoxystyrene) (PAS), we found that PVPh/PAS polymer blends are immiscibile because the self-associative hydrogen bonding of the PVPh component is more favorable than the inter-associative hydrogen bonding between PVPh and PAS segments due to the strong intramolecular screening effect in this binary blend system. The incorporation of a styrene moiety (diluent segment) into the PVPh main chain is able to enhance its miscibility with PAS due to the decrease of the strong self-association in the PVPh component in the PVPh/PAS blend.[28] The aim of this study is to explore the effect of resonance on self- and inter-associative hydrogen bonding of poly(methacrylamides) with different N-substitution (i.e., methyl, cyclohexyl, and phenyl) by blending with poly(4-vinylpyridine) (P4VP). The specific hydrogen bonding interaction between the amide carbonyl and pyridine groups competes with self-association of amide groups. The main purpose of this study is to explore the difference of self- and inter-associative hydrogen-bond behaviors between P4VP and poly(methacrylamides) with different N-substitutions and the effects of resonance of aromatic groups upon the miscibility.

Experimental Section

Materials. *N*-Methyl methacrylamide and *N*-phenyl methacrylamide were purchased from TCI Chemical Company which were purified by column chromatography and recrystallized before use. Poly(4-vinyl pyridine) (P4VP) was purchased from Aldrich Chemical. The radical initiator azobisisobutyronitrile (AIBN) was recrystallized from ethyl alcohol prior to use. Toluene was distilled under a vacuum and then used as the solvent for the polymerization. Methacryloyl chloride and cyclohexyl amine were used as received without further purification.

Synthesis. ***Synthesis of N-Cyclohexyl Methacrylamide.*** *N*-Cyclohexyl amine (0.05 mol), triethylamine (TEA, 0.05 mol), and 50 mL of dried THF were fed in a 250 mL round-bottom flask equipped with a magnetic stirrer, dropping funnel, and thermometer. The reaction mixture was cooled to 0−4 °C, 0.06 mol of methacryloyl chloride in dried THF (20 mL) was added dropwisely to the reaction mixture over a period of 0.5 h, and the reaction mixture was stirred for 24 h at room temperature. After removing the formed solid quaternary ammonium salt, the solution was washed thoroughly with 5 wt % sodium hydroxide solution, dilute hydrochloric acid, and water, and then dried over anhydrous magnesium sulfate. After evaporation of the solvent, white *N*-cyclohexyl methacrylamide was obtained and purified by recrystallization. ^{1}H NMR ($CDCl_3$, ppm): 1−1.8 (10H, cyclohexyl), 1.90 (3H, methyl), 3.7 (1H, N—CH), 5.22 and 5.59 (2H, C═CH_2).

Synthesis of Poly(N-methyl methacrylamide), Poly(N-cyclohexyl methacrylamide), and Poly(N-phenyl methacrylamide). AIBN (1 wt % based on monomers) was used for the degassed solution of *N*-methyl methacrylamide in toluene at 80 °C under a nitrogen atmosphere in a glass reaction flask equipped with a condenser. The mixture was stirred for ca. 36 h and poured into excess hexane under vigorous agitation to precipitate the crude poly(*N*-methyl methacrylamide) product. The crude product was purified by redissolving in toluene and

TABLE 2: Molar Volume, Molecular Weight, and T_g of the Four Homopolymers Employed in This Study[a]

polymer	V^b	M_w	T_g (°C)
PNMAA	84.5	1800	255
PNCHAA	147.2	2000	149
PNPAA	128.2	1600	201
P4VP	84.5	60000	152

[a] V, molar volume (mL/mol); M_w, molecular weight (g/mol). [b] Obtained by the molar volume group contribution method.[31]

TABLE 3: T_g Behaviors of PNMAA/P4VP, PNCHAA/P4VP, and PNPAA/P4VP Blends with Different Compositions

composition (amide/pyridine)	T_g (°C) PNMAA/P4VP	PNCHAA/P4VP	PNPAA/P4VP
100/0	255	149	201
90/10		165	190
75/25	152/256	170	200
50/50	154/252	169	210
25/75	160/250	168	211
10/90	158/246		
0/100		152	

then added dropwisely into a large excess of hexane. This procedure was repeated several times, and then, the residual solvent of the final product was removed under a vacuum at 70 °C for 1 day to yield pure white poly(*N*-methyl methacrylamide). Table 2 summarizes molecular weight, T_g, and molar volume values[31] of these four homopolymers employed in this study.

Polymer Blending. Poly(methacrylamides)/P4VP blends with various compositions were prepared by solution casting. The tetrachloroethane solution containing about 10 wt % polymer mixtures was stirred for 24 h, and the solution was allowed to evaporate slowly at 60 °C for 1 day. The blend was then dried at 120 °C for 1 week to remove the residual solvent.

Characterizations. The glass transition temperature of the copolymer was determined using a Du-Pont DSC-9000 DSC system. The sample was kept at 250 °C for 1 min and then cooled quickly to 30 °C from the melt of the first scan. The value of T_g was obtained as the inflection point of the jump heat capacity at a scan rate of 20 °C/min within the temperature range 25−280 °C. All measurements were conducted under a nitrogen atmosphere. Molecular weights and molecular weight distributions were determined by matrix-assisted laser desorption/ionization time-of-flight mass spectrometry (MALDI-TOF-MS). Infrared spectra of the copolymer films were determined by using the conventional NaCl disk method. The tetrachloroethane solution containing the blend was cast onto a NaCl disk. The film used in this study was thin enough to obey the Beer−Lambert law. FTIR measurements were performed on a Nicolet Avatar 320 FTIR spectrophotometer; 32 scans were collected at a spectral resolution of 1 cm^{-1}. ^1H NMR spectra of these homopolymers were recorded on a Bruker ARX300 spectrometer using $CDCl_3$ as the solvent. High-resolution solid-state ^{13}C NMR spectroscopy experiments were performed at 25 °C using a Bruker DSX-400 spectrometer operating at a resonance frequency of 100.47 MHz. High-resolution solid-state ^{13}C NMR spectra were acquired using the cross-polarization (CP)/magic-angle spinning (MAS)/high-power dipolar decoupling (DD) technique, with a 90 °C pulse width of 3.9 μs, a pulse delay time of 3 s, an acquisition time of 30 ms, and 2048 scans. A magic-angle sample-spinning rate of 5.4 kHz was used to avoid absorption overlapping. The proton spin−lattice relaxation time in the rotating frame ($T_{1\rho}^H$) was determined indirectly via carbon observation using a 90 °C τ-spin lock pulse sequence prior to CP. The data acquisition was performed at delay times (τ) ranging from 0.1 to 10 ms with a contact time of 1.0 ms.

Results and Discussion

Thermal Analyses. Differential scanning calorimetry (DSC) is one of the convenient methods to determine the miscibility in polymer blends. Figure 4 displays the second run DSC thermograms of all blends of PNMAA, PNCHAA, and PNPAA with P4VP at various compositions, and their T_g's are summarized in Table 3. Clearly, PNMAA/P4VP blends are immiscible based on DSC analyses, since all of the compositions of these two blends show two glass transition temperatures, indicating less effective inter-associative hydrogen bonding between the amide group of PNMAA and the pyridine group of P4VP. Two clear T_g's are observed for the compositions, and the values of lower and higher T_g correspond to P4VP-rich and PNMAA-rich, respectively.

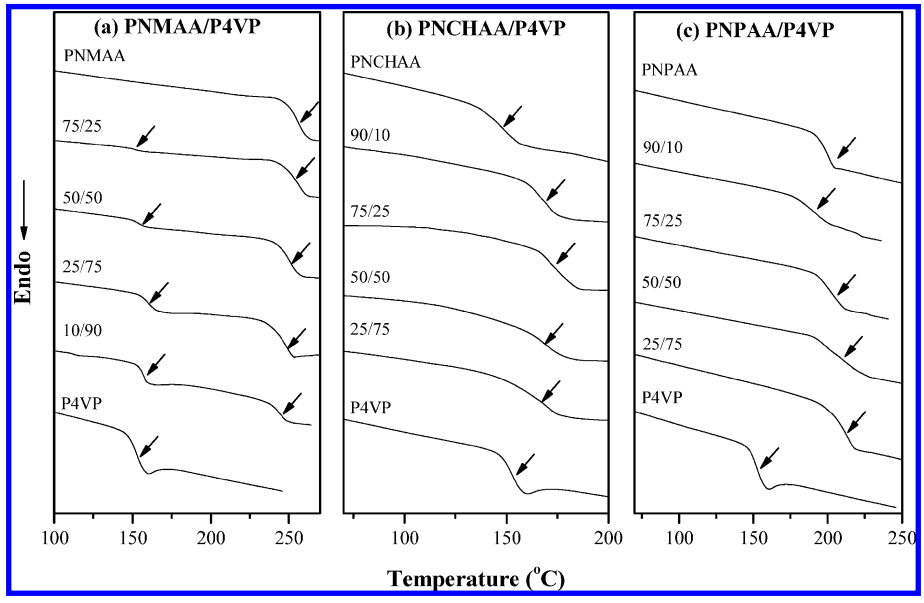

Figure 4. DSC scans of (a) PNMAA/P4VP, (b) PNCHAA/P4VP, and (c) PNPAA/P4VP blends with different compositions.

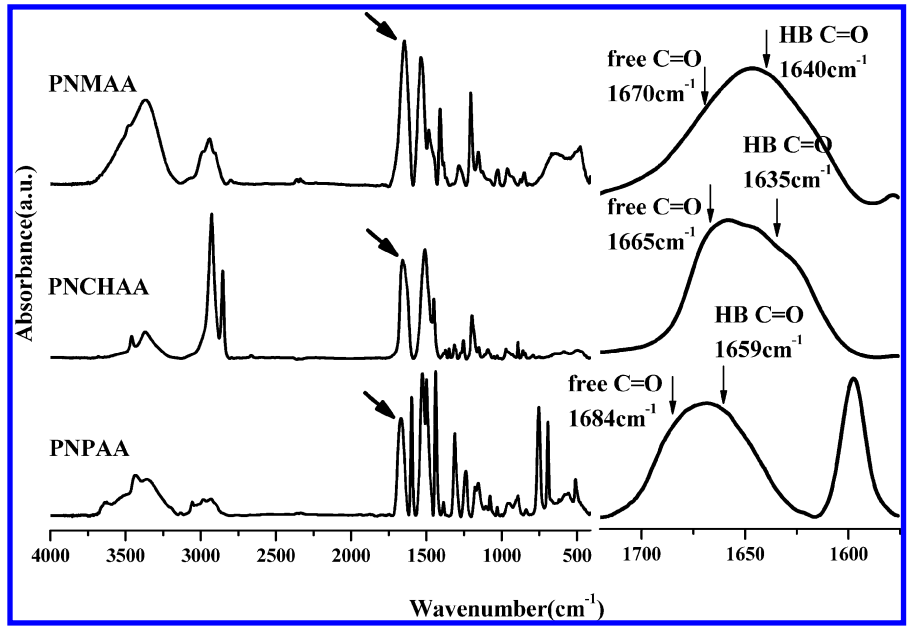

Figure 5. FTIR spectra for three neat polymethacrylamides: PNMAA, PNCHAA, and PNPAA.

In PNCHAA/P4VP blends (as shown in Figure 4b), all blends show a single glass transition temperature, indicating that there is more effective inter-associative hydrogen bonding between PNCHAA and P4VP than that of PNMAA/P4VP. Furthermore, all PNPAA/P4VP blends also show a single glass transition temperature (as shown in Figure 4c), indicating that the incorporation of a bulky side group into the poly(methacrylamides) is able to enhance its miscibility with P4VP due to the decrease of the strong self-association in the poly(methacrylamides) component that will be discussed in FTIR analyses.

Strength of Specific Interaction, as Determined by FTIR Spectroscopy. ***Qualitative Analysis of Experimental Observation.*** FTIR spectroscopy has been proven to be a powerful technique to detect the presence of self-association within a given molecule and inter-association between two chemically dissimilar molecules. Figure 5 shows FTIR spectra recorded at room temperature for these three neat poly(methacrylamides) and scale-expanded FTIR spectra in the region of the carbonyl stretching vibration. Two carbonyl stretching bands in PNMAA were obtained by a curve-fitting procedure:[32] one centered at 1670 cm^{-1} and another centered at 1640 cm^{-1}, corresponding to free and self-association hydrogen-bonded carbonyl groups, respectively.[33] Figure 6 shows scale-expanded (second-derivate) infrared spectroscopy of the PNCHAA in the range 1580−1710 cm^{-1} and the PNPAA in the range 1610−1720 cm^{-1}. Clearly, the two main minima under zero-point line (dashed line) in the second-derivative spectra shown in Figure 6a of PNCHAA are observed for (1) the free carbonyl group units at 1665 cm^{-1} and (2) the self-associated, hydrogen-bonding carbonyl groups at 1635 cm^{-1}. The peak positions of free and hydrogen-bonded carbonyl groups are similar to those in PNMAA. In PNPAA, the two main minima under zero-point line in the second-derivative spectra shown in Figure 6b of PNPAA are observed for (1) the free carbonyl groups unit at 1684 cm^{-1} and (2) the self-associated, hydrogen-bonding carbonyl groups at 1659 cm^{-1}. There were good correlations between the experimental spectra and theoretical fitting of the results.[34,35] However, because of broad second derivatives in the 1610−1720 cm^{-1} region, it seems that there are three carbonyl stretching bands: one is corresponding to the free carbonyl band, and the others are corresponding to the hydrogen-bonded carbonyl bands. There

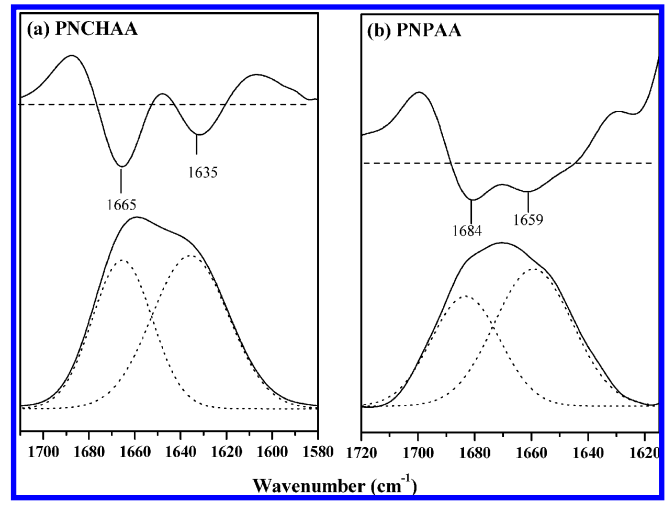

Figure 6. IR spectrum at the carbonyl stretching region and its second derivative spectrum of (a) PNCHAA and (b) PNPAA.

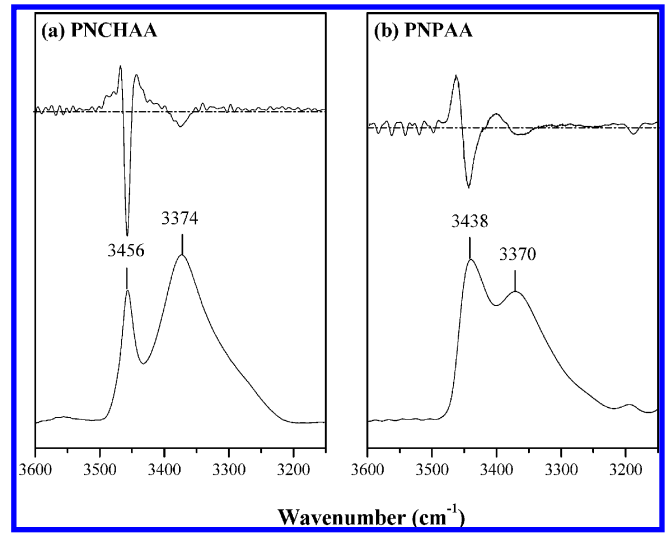

Figure 7. IR spectrum recorded at 120 °C of the NH stretching region for (a) PNCHAA and (b) PNPAA.

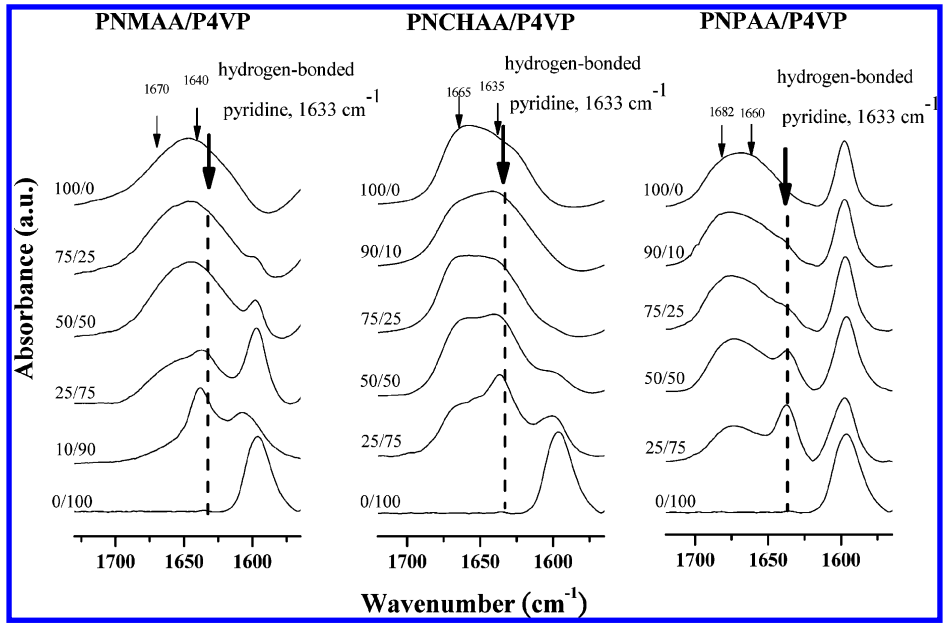

Figure 8. FTIR spectra at room temperature for (a) PNMAA/P4VP blends, (b) PNCHAA/P4VP blends, and (c) PNPAA/P4VP blends.

are two possibilities: one is that there is an additional hydrogen-bonded dimer band as well as a multimer band, but the steric bulky aromatic group in PNPAA makes multimer formation difficult.[32] The steric factor equally affects PNCHAA, but PNCHAA does not have an aromatic ring; in addition, there are two clear minima under zero-point line in the second-derivative spectra shown in Figure 6a of PNCHAA. Thus, the possibility of a steric factor can be excluded. Alternatively, Choperena et al. reported that the π-orbitals on the aromatic ring can form weak hydrogen bonding with the O−H group in PVPh.[36] In the FTIR spectra in the N−H stretching region for PNCHAA and PNPAA recorded at 120 °C, as shown in Figure 7, the second derivative of PNPAA shows a slightly more broad peak at lower frequency which is corresponding to the self-associated band, indicating that the π-orbitals on the aromatic ring in PNPAA are able to form a self-associated hydrogen bond with the N−H group. However, the hydrogen-bond acceptor ability of the carbonyl group compares much higher with that of the π-orbitals on the aromatic ring.[37] It is too complicated to resolve the self-associative hydrogen bonding with relatively weak aromatic···H−N bonding. As a result, the self-associated aromatic···H−N bonding in PNPAA is ignored to simplify the system in this study.

These results of PNPAA are different from those in PNMAA and PNCHAA. Moreover, Zhang et al.[38] pointed out that the difference in wavenumber ($\Delta\nu_H$) between the absorption bands of hydrogen-bonded and free pyridine groups could be used as a measure of the relative strength of hydrogen bonding, so the difference in wavenumber ($\Delta\nu_H$) between the absorption peaks of hydrogen-bonded and free carbonyl group in PNPAA is smaller than that in PNMAA and PNCHAA, indicating that the relative strength of self-association hydrogen bonding in PNPAA is smaller than that in PNMAA and PNCHAA. The phenyl group makes the carbonyl stretching characteristics of PNPAA different from those in PNMAA and PNCHAA.

Figure 8 gives FTIR spectra of the carbonyl and pyridine vibrations region for P4VP-based blends. Upon mixing P4VP with PNMAA, a new band at 1633 cm^{-1} is observed (see Figure 8a), which is characteristic of the inter-association of pyridine−amide interaction. In PNMAA/P4VP and PNCHAA/P4VP blends, the absorption band of hydrogen-bonded pyridine is more obvious in the composition of 25/75; however, the absorption band of hydrogen-bonded pyridine is clear in all compositions in PNPAA/P4VP blends, indicating that the fraction of hydrogen-bonded pyridine in PNPAA/P4VP blends is higher than that in PNMAA and PNCHAA. Moreover, unlike self-associative interaction of poly(methacrylamides), the peak positions of hydrogen-bonded pyridine in three poly(mathacrylamides)/P4VP blends are almost the same, no matter what the N-substitution is, indicating the strength of inter-associative hydrogen bonding is similar in these three binary blends.

Quantitative Analysis of Experimental Results via the Painter−Coleman Association Model. The Painter−Coleman association model[31] can be used to describe the thermodynamics of polymer blends with hydrogen bonding, which can be written using the following scheme: where B_1 represents the amide-

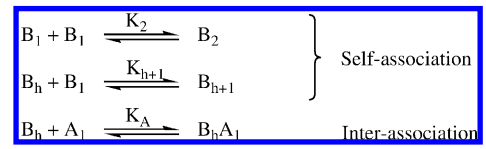

NH group, A_1 represents the pyridine group, B_2 is the hydrogen-bonded dimer formed between two amide groups, B_h is the hydrogen-bonded multimer, and B_hA_1 is the inter-associative hydrogen bonding.

The change in the relative intensities of the free and hydrogen-bonded carbonyl bands varies systematically in favor of the former as temperature increasing, as shown in Figure 9, reflecting the decreasing fraction of hydrogen-bonded carbonyl groups present as a function of temperature. This is a measure of the enthalpy of hydrogen bond formation. The methodology employed to determine the enthalpy of hydrogen bond formation from infrared spectra has been discussed in detail in previous publications.[32,39] The equilibrium constant K_B of self-association of amide groups is related to the $f_F^{C=O}$ values through

$$K_B = \frac{1 - f_F^{C=O}}{[f_F^{C=O}]^2} \quad (1)$$

and the K_B at different temperatures could be calculated.

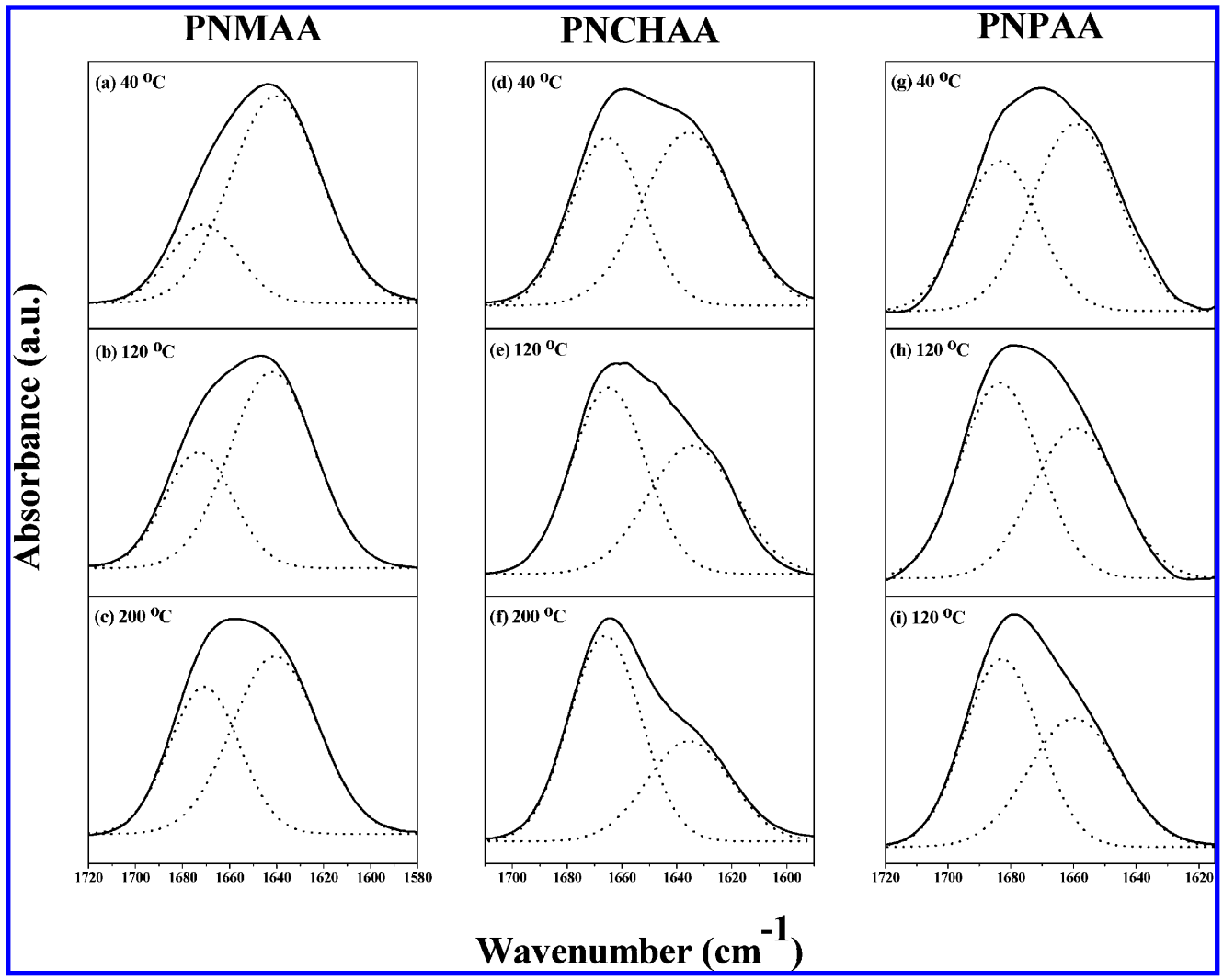

Figure 9. Infrared spectra and curve-fitting results of (a) PNMAA, (b) PNCHAA, and (c) PNPAA recorded at different temperatures in the region 1575−1720 cm^{-1}.

Polymer blends with hydrogen bonding acceptor can be summarized as follows:

$$\phi_B = \frac{\phi_{B_1}}{(1 - K_B\phi_{B_1})^2}\left[1 + \frac{K_A\phi_{A_1}}{r}\right] \quad (2)$$

$$\phi_A = \phi_{A_1}\left[1 + \frac{K_A\phi_{B_1}}{(1 - K_B\phi_{B_1})}\right] \quad (3)$$

where ϕ_B and ϕ_A are the volume fractions of components B and A, respectively, in the blend, ϕ_{B_1} and ϕ_{A_1} are the volume fractions of free B and A groups, respectively, and $r = V_A/V_B$, with V_A and V_B respectively being the molar volumes of components A and B. K_B and K_A appearing in eqs 1 and 2 are equilibrium constants, the definitions of which in terms of the hydrogen-bonded components can be determined from FTIR spectroscopic measurements. The fraction of carbonyl group in amide units that are free is given by

$$f_F^I = (1 - K_B\phi_{B_1}) \quad (4)$$

and the fraction of free carbonyl groups is equal to the number of chains that do not have a pyridine unit attached to one end, divided by the total number of amide units present; we can obtain

$$f_F^{II} = \frac{(1 - K_B\phi_{B_1})}{\left(1 + \frac{K_A\phi_{A_1}}{r}\right)} \quad (5)$$

Finally, the fraction of free is simply the number of non-hydrogen-bonded pyridine groups divided by the total number of pyridine groups and, converting to volume fractions, we obtain:

$$f_F^{III} = \frac{\phi_{A_1}}{\phi_A} \quad (6)$$

Obviously, the equilibrium constants and hence the stoichiometry of hydrogen boning varied with temperature. This is simply described through the usual dependence on the enthalpy of hydrogen bond formation:

$$K_B = K_B^\circ \exp\left[-\frac{\Delta h_B}{R}\left(\frac{1}{T} - \frac{1}{T^\circ}\right)\right] \quad (7)$$

$$K_A = K_A^\circ \exp\left[-\frac{\Delta h_A}{R}\left(\frac{1}{T} - \frac{1}{T^\circ}\right)\right] \quad (8)$$

where K_B° and K_A° are the values of the equilibrium constants determined at T° K (usually 298 K), R is the universal gas constant, and Δh_i is the molar enthalpy of the formation of individual hydrogen bonds. Using eqs 7 and 8, we can calculate the equilibrium constants at different temperatures.

Let us pay attention in advance to self-associative hydrogen bonding in poly(methacrylamides). Figure 9 shows scale-expanded FTIR spectra of three pure poly(methacrylamides) in the region from 1575 to 1720 cm^{-1} at different temperatures from 40 to 220 °C. The curve-fitting limits were set to 1560−1740 cm^{-1}, and the spectra were curve resolved into two bands using a lease-squares fitting procedure.[37] Lorenztian band shapes were fixed, the ν of the two bands in PNMAA were restricted to ranges of 1670 ± 1 and 1640 ± 1 cm^{-1}, and $w_{1/2}$ was restricted to the range from 34.5 ± 1 to 43.0 ± 1 cm^{-1}, respectively, for all of the least-squares fits. A value of $a_{HB}/a_F = 1.2$ is employed to calculate the fraction of free and hydrogen-bonded carbonyl groups.[32] The calculations of K_B for the different temperatures are listed in the final column of Table 4. A van't Hoff plot of ln K_B versus the reciprocal of temperature is shown in Figure 10, and we can obtain a value of 2.22 kcal/mol for the enthalpy Δh_B of hydrogen bond formation from the slope of least-squares linear fit of the data in Table 6. The same methodology was employed to calculate the enthalpy of hydrogen bond formation of PNPAA and PNCHAA, with the values of 1.29 and 2.17 kcal/mol, respectively.

Here, we turn our attention to inter-associative hydrogen bonding in poly(methacrylamide)/P4VP blends. The numerical values of parameters necessary for the calculations of various quantities described above are summarized in Table 2, which are taken from the literature.[31,32] Except free carbonyl and hydrogen-bonded carbonyl groups in poly(methacrylamides), the temperature-dependent band in FTIR spectra of poly(methacrylamide)/P4VP blends could correspond with the pyridine group in P4VP. In Figure 8, the band at 1633 cm^{-1} in PNMAA/P4VP, PNCHAA/P4VP, and PNPAA/P4VP blends, which is characteristic of the hydrogen-bonded pyridine group, could be used to calculate the equilibrium constants K_A at variable temperature by eqs 2−8. Figure 11 shows scale-expanded FTIR spectra and curve-fitting peaks of three poly(methacrylamide)/P4VP compositions of 50/50 in the region from 1560 to 1730 cm^{-1} at 40, 120, and 200 °C, and all of the curve-fitting results and the calculations of K_B for the different temperatures are listed in Table 5. Again, a van't Hoff plot of ln K_A versus the reciprocal of temperature is shown in Figure 12, and we can obtain values of 3.24, 3.26, and 3.22 kcal mol^{-1} for the enthalpy Δh_A of inter-associative hydrogen-bond formation of PNMAA/P4VP, PNPAA/P4VP, and PNCHAA/P4VP blends, respectively, from the slope of least-squares linear fit of the data in Table 5.

Solid-State NMR Spectroscopy. In addition to FTIR, evidence on interactions in the blends can also be obtained from solid-state NMR spectroscopy, as demonstrated by changes in chemical shift and/or line shape. Figure 13 shows the selected ^{13}C CP/MAS spectra of various PNCHAA/P4VP and PNPAA/P4VP blends. Five peaks are also observed for pure P4VP where the peak at $\delta = 123.9$ ppm corresponds to the pyridine carbon atom (C-12). Pure PNCHAA and PNPAA display eight peaks

TABLE 4: Curve Fitting of the Fraction of Free and Hydrogen-Bonded Carbonyl Group of PNMAA, PNPAA, and PNCHAA

temp	PNMAA			PNCHAA			PNPAA		
(°C)	f_F (%)	f_b (%)	K_B	f_F[a] (%)	f_b (%)	K_B	f_F[b] (%)	f_b (%)	K_B
40	24.4	75.4	12.5	47.5	52.5	2.32	45.6	54.4	2.61
60	26.4	73.6	10.5	50.8	49.2	1.90	47.6	52.4	2.32
80	28.8	71.2	8.6	53.8	46.2	1.60	49.0	51.0	2.12
100	30.3	69.7	7.6	56.7	43.3	1.35	50.5	49.5	1.94
120	32.8	67.2	6.2	59.2	40.8	1.16	52.3	47.7	1.75
140	34.4	65.6	5.5	61.2	38.8	1.04	53.7	46.3	1.60
160	35.9	64.1	5.0	63.3	36.7	0.92	55.6	44.4	1.44
180	37.9	62.2	4.4	65.1	34.9	0.82	56.2	43.8	1.38
200	40.2	59.8	3.7	67.1	32.9	0.73	57.7	42.3	1.27
220	41.3	58.7	3.4	69.0	31.0	0.65	58.1	41.9	1.24

[a] The ν of the two bands were restricted to ranges of 1665 ± 1 and 1635 ± 1 cm^{-1}, and the $w_{1/2}$ was restricted to ranges of 31.0 ± 1 and 36.0 ± 1 cm^{-1}, respectively. [b] The ν of the two bands were restricted to ranges of 1684 ± 1 and 1659 ± 1 cm^{-1}, and the $w_{1/2}$ was restricted to ranges of 27.0 ± 1 and 34.0 ± 1 cm^{-1}, respectively.

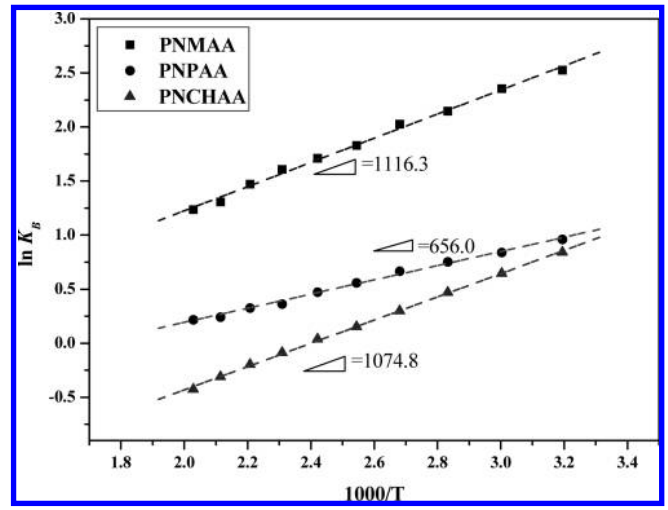

Figure 10. van't Hoff plot of ln K_B versus reciprocal temperature for PNMAA, PNCHAA, and PNPAA.

where the C=O carbonyl group is at 177.5 and 176.3 ppm, respectively. All other peaks are also assigned in Figure 13. Clearly, the pyridine carbons (C-12) shift downfield about 2.1 ppm significantly also indicating that the hydrogen bonding interaction between the amide group of PNCHAA and PNPAA the pyridine group of P4VP, this finding is consistent with the results of our FTIR spectroscopic analysis.

Solid-state NMR spectroscopy also has been used to better understand the phase behavior and miscibility of polymer blends. A single T_g based on DSC analysis implies that the mixing of two blending components is in a scale of about 20−40 nm.[10] The dimension of mixing smaller than 20 nm can be obtained through measurement of the spin−lattice relaxation time in the rotating frame ($T_{1\rho}^H$).[10] The $T_{1\rho}^H$ values of the blends were measured through the delayed-contact ^{13}C CP/MAS experiments. The ($T_{1\rho}^H$) values are calculated from eq 9:

$$\ln(M_\tau/M_0) = -\tau/T_{1\rho}^H \quad (9)$$

where τ is the delay time used in the experiment and M_τ is the corresponding resonance. Figure 14 present the values of $-\ln(M_\tau/M_0)$ plotted against τ of PNCHAA/P4VP blends. We estimated the homogeneities of these polymer blends through

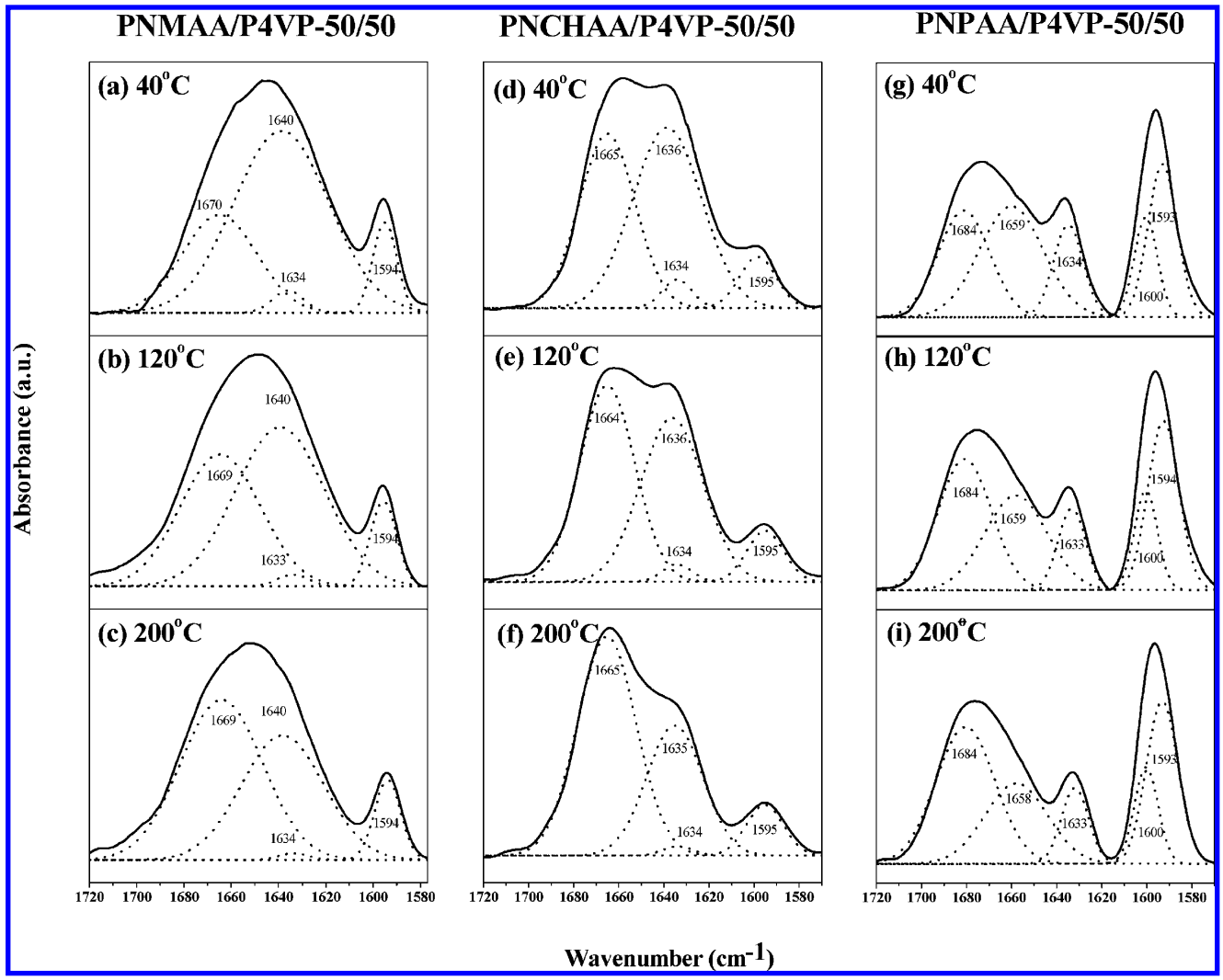

Figure 11. Scale-expanded infrared spectra and curve-fitting results of (a) PNMAA/P4VP-50/50, (b) PNPAA/P4VP-50/50, and (c) PNCHAA/P4VP-50/50, from 1570 to 1720 cm^{-1} at 40, 120, and 200 °C.

TABLE 5: Curve Fitting of the Fraction of Free and Hydrogen-Bonded Carbonyl and Pyridine Groups in PNMAA/P4VP, PNCHAA/P4VP, and PNPAA/P4VP Compositions of 50/50

	PNMAA/P4VP				PNCHAA/P4VP				PNPAA/P4VP			
	the fraction of free C=O and free pyridine				the fraction of free C=O and free pyridine				the fraction of free C=O and free pyridine			
temp (°C)	f_F^{Ia} (%)	f_F^{IIb} (%)	f_F^{IIIc} (%)	K_A	f_F^{I} (%)	f_F^{II} (%)	f_F^{III} (%)	K_A	f_F^{I} (%)	f_F^{II} (%)	f_F^{III} (%)	K_A
40	0.178	0.074	0.396	85.3	0.240	0.088	0.348	57.5	0.238	0.045	0.308	151.8
60	0.196	0.100	0.403	60.1	0.251	0.111	0.360	42.8	0.246	0.062	0.316	105.3
80	0.205	0.118	0.413	47.9	0.258	0.133	0.375	33.0	0.250	0.079	0.328	77.4
100	0.220	0.143	0.423	37.4	0.272	0.163	0.390	24.7	0.261	0.097	0.336	60.2
120	0.236	0.172	0.436	28.7	0.280	0.185	0.406	20.1	0.274	0.117	0.340	47.8
140	0.247	0.195	0.448	23.5	0.291	0.205	0.415	17.2	0.292	0.136	0.345	39.8
160	0.266	0.223	0.456	19.5	0.312	0.232	0.421	14.4	0.308	0.153	0.349	35.0
180	0.282	0.244	0.462	17.0	0.332	0.263	0.431	11.8	0.321	0.176	0.354	28.6
200	0.303	0.268	0.465	14.9	0.339	0.286	0.449	9.9	0.329	0.191	0.361	25.2
220	0.322	0.296	0.474	12.5	0.351	0.308	0.458	8.6	0.346	0.214	0.368	21.4

[a] f_F^I is the fraction of carbonyl groups in amide units that are free. [b] f_F^{II} is the fraction of free carbonyl groups that do not have a pyridine unit attached to one end. [c] f_F^{III} is the fraction of non-hydrogen-bonded pyridine groups.

quantitative analyses based on the PNCHAA-carbon (C-5) atom's resonance at 46 ppm and the P4VP-carbon (C-9) atom's resonance at 40 ppm. From the slopes of the fitted lines, we determined the values of $T_{1\rho}^H$, which are listed in Table 6, for various compositions of PNCHAA/P4VP and PNPAA/P4VP blends. From DSC scans, PNCHAA/P4VP blends show a single glass transition temperature; however, all PNCHAA/P4VP compositions display heterogeneous non-single-exponential behavior, indicating that these blends are not homogeneous on the scale at which spin diffusion occurs within the time $T_{1\rho}^H$.

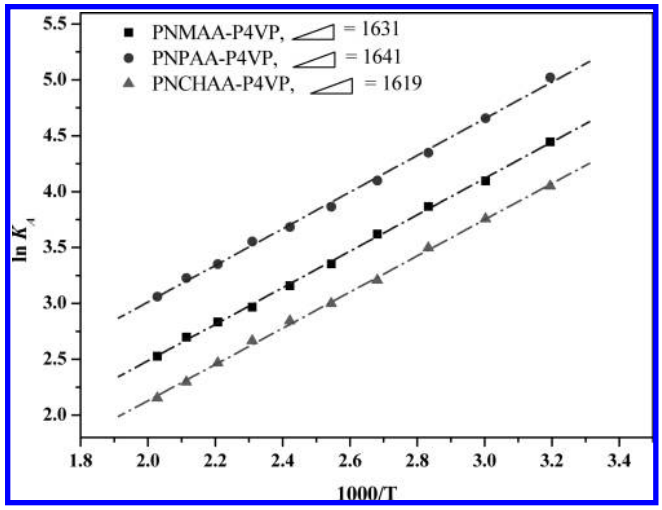

Figure 12. van't Hoff plot of ln K_A versus reciprocal temperature for PNMAA/P4VP, PNCHAA/P4VP, and PNPAA/P4VP blends.

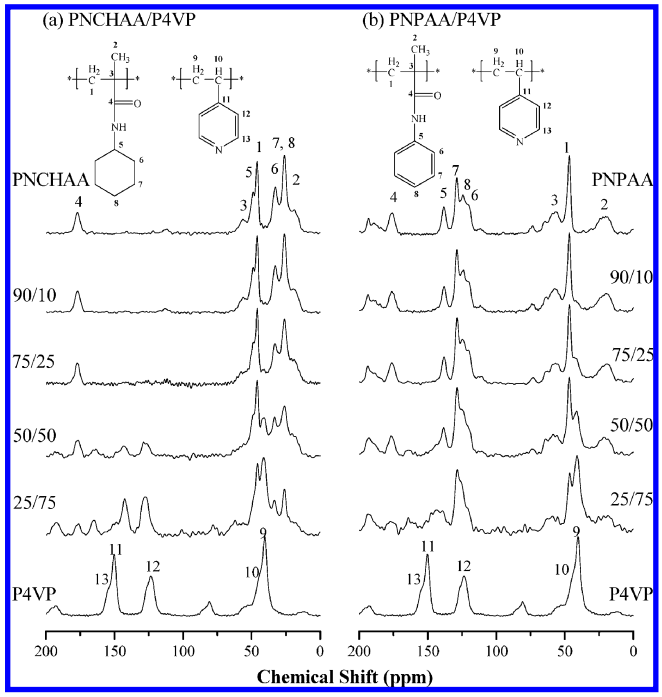

Figure 13. ^{13}C CP/MAS spectra of (a) PNCHAA/P4VP and (b) PNPAA/P4VP blends.

There are two domains, with distinct mobility, present in this blend on a scale below 20 nm.[40,41]

Figure 15 presents the values of $-\ln(M_\tau/M_0)$ plotted against τ of PNPAA/P4VP blends, and the values of $T_{1\rho}{}^H$ are listed in Table 6. The homogeneities of these polymer blends are estimated through quantitative analyses based on the PNPAA-carbon (C-1) atom's resonance at 46 ppm and the P4VP-carbon (C-9) atom's resonance at 40 ppm. We obtained single-exponential decays in $T_{1\rho}{}^H$ of the P4VP-carbon (C-9) atom's resonance at 40 ppm for all of the PNPAA/P4VP compositions, suggesting that these blends are homogeneous on the scale at which spin diffusion occurs within the time $T_{1\rho}{}^H$. Moreover, the $T_{1\rho}{}^H$ decays at 40 ppm of these two compositions are much smaller than the $T_{1\rho}{}^H$ decay of pure P4VP, and the composition of 25/75 shows a shorter $T_{1\rho}{}^H$ relaxation time than that of the composition of 75/25. The shorter $T_{1\rho}{}^H$ relaxation time that the blend attained reflects the rigid nature of the blend, indicating that more addition of P4VP creates more or stronger inter-associative interaction between two components in the composition of 25/75. Thus, the PNPAA/P4VP composition of 25/75 shows a higher T_g value than that of the composition of 75/25.

The reason for these results of DSC, FTIR, and solid-state NMR analysis is mainly due to the electron delocalization effect. The phenyl group and cyclohexyl group are both more bulky than the methyl group, and the steric hindrance of the side-chain group in PNPAA and PNCHAA prevents the formation of hydrogen bonds.[42] Thus, the equilibrium constants K_B at 40 °C of self-associative hydrogen bonding of PNPAA and PNCHAA are comparable to each other, and both of them are smaller than the K_B of PNMAA at 40 °C.[43] However, Figure 10 also shows the smaller slope of PNPAA than PNCHAA and PNMAA, indicating that steric bulk is not the factor to make a different enthalpy of self-associative hydrogen bonding of PNPAA from PNCHAA and PNMAA. The hydrogen-bonding strength of PNCHAA is stronger than that of PNPAA. The difference between PNPAA and PNCHAA is the resonance characteristics of PNPAA, and the resonance characteristics are also the absence of both PNMAA and PNCHAA. Comparing the free carbonyl group in PNMAA, PNPAA, and PNCHAA, the absorption frequency of the free carbonyl group in PNPAA is higher than that in PNMAA and PNCHAA, indicating that the aromatic group makes the carbonyl group in PNPAA more electrodeficient than the carbonyl group in PNMAA and PNCHAA.[44] The aromatic ring in PNPAA makes the carbonyl

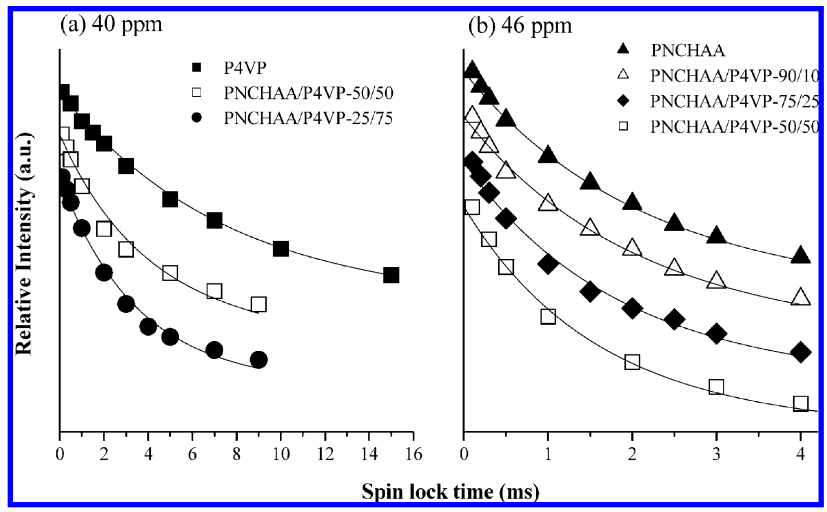

Figure 14. Solid-state NMR spectroscopic $T_{1\rho}{}^H$ decay curves for PNCHAA/P4VP blends with different compositions at (a) 40 ppm of the P4VP-ethylene-carbon atom's resonance and (b) 46 ppm of the PNCHAA-ethylene-carbon atom's resonance.

TABLE 6: Values of $T_{1\rho}^{H}$ of the Pure PNCHAA, Pure PNPAA, Pure P4VP, and Various Compositions of PNCHAA/P4VP and PNPAA/P4VP Blends

	$T_{1\rho}^{H}$ (ms)			
	PNCHAA/P4VP		PNPAA/P4VP	
composition amide/pyridine	PNCHAA-ethylene, 46 ppm	P4Vp, 40 ppm	PNPAA-ethylene, 47 ppm	P4VP-ethylene, 40 ppm
100/0	2.54		4.14	
90/10	1.41/2.50		4.15	
75/25	1.37/2.42		3.86	4.99
50/50	1.35/2.30	3.23/7.22	3.64	4.09
25/75		3.19/7.02		3.40
0/100		7.57		7.57

group electron-deficient, resembling an electron-withdrawing group, so that the carbonyl group in PNPAA has a poorer ability to form a hydrogen bond with a smaller enthalpy of self-associative hydrogen bond formation.

However, in polymethacrylamide/P4VP blends, all of the PNPAA/P4VP compositions show single T_g and single-exponential decays in $T_{1\rho}^{H}$, indicating that there is more effective inter-associative hydrogen bonding between the amide group of PNPAA and the pyridine group of P4VP. In Figure 11, the fraction of hydrogen-bonded pyridine in PNPAA/P4VP blends is larger than those in PNMAA/P4VP and PNCHAA/P4VP blends, although the enthalpy of inter-associative hydrogen bond formation from the van't Hoff plot and the difference in wavenumber ($\Delta\nu_H$) between the absorption peaks of hydrogen-bonded and free pyridine group are similar to each other in these three polymethacrylamide/P4VP blends. From the curve-fitting results at 40 °C in Table 5, the value of f_F^I in PNPAA/P4VP is comparable to that in PNCHAA/P4VP but smaller than that in PNMAA/P4VP, indicating that the total number of hydrogen bonds in PNPAA/P4VP, regardless of self- or inter-association, is comparable to that in PNCHAA/P4VP but less than that in PNMAA/P4VP. However, the value of f_F^{III} in PNPAA/P4VP is smaller than that in PNMAA/P4VP and PNCHAA/P4VP, and the value of f_F^{II} in PNPAA/P4VP is smaller than that in PNMAA/P4VP and PNCHAA/P4VP. As a result, the fraction of inter-association in PNPAA/P4VP is larger than that in PNMAA/P4VP and PNCHAA/P4VP blends. All of these results indicate that resonance characteristics of PNPAA can increase the amount of inter-associative hydrogen bonding between PNPAA and P4VP to enhance the miscibility of PNPAA/P4VP blends but cannot affect the strength of inter-association hydrogen-bond formation.

Because of intramolecular screening effects, forming inter-association between two components will lose internal degree of rotational freedom (i.e., rotations around backbone bonds) and change the entropy in a binary blending system,[45] so self-association is preferred to inter-association, except appearing a driving force. Table 7 lists the ratios of the equilibrium constants of inter-association (K_A) and self-association (K_B) at 40 and 220 °C, and the ratio of the enthalpy of inter-association (Δh_A) and self-association (Δh_B). Larger Δh_A than Δh_B cannot ensure a miscible

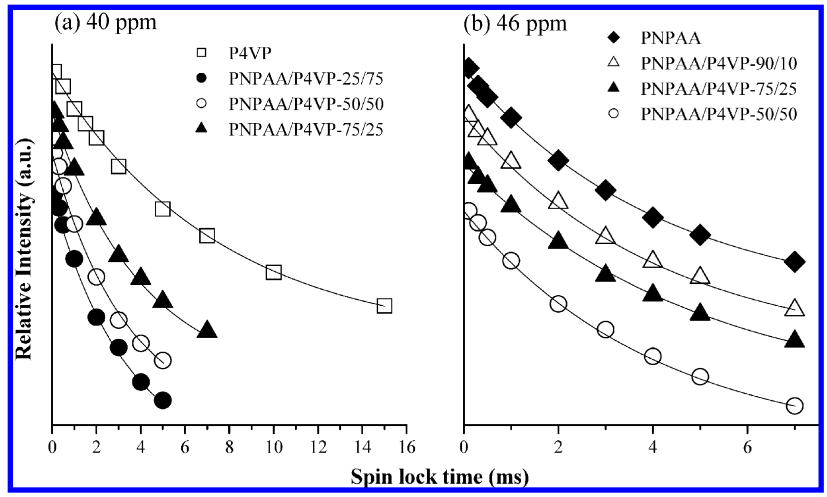

Figure 15. Solid-state NMR spectroscopic $T_{1\rho}^{H}$ decay curves for PNPAA/P4VP blends with different compositions at (a) 40 ppm of the P4VP-ethylene-carbon atom's resonance and (b) 46 ppm of the PNPAA-ethylene-carbon atom's resonance.

TABLE 7: Ratios of the Equilibrium Constants of Inter- and Self-Association and Ratios of the Enthalpy of Inter- and Self-Association in Three Polymethacrylamide/P4VP Blends

	PNMAA/P4VP			PNCHAA/P4VP			PNPAA/P4VP		
temp (°C)	K_A[a]	K_B	K_A/K_B	K_A	K_B	K_A/K_B	K_A	K_B	K_A/K_B
40	85.3	12.5	6.8	57.5	2.3	24.8	151.8	2.6	58.4
220	12.5	3.4	3.7	8.6	0.65	13.2	21.4	1.2	17.8
enthalpy (kcal/mol)	$\Delta h_A = 3.24$			$\Delta h_A = 3.22$			$\Delta h_A = 3.26$		
	$\Delta h_B = 2.22$			$\Delta h_B = 2.17$			$\Delta h_B = 1.29$		

[a] K_B is the self-association equilibrium constant, K_A is the inter-association equilibrium constant, Δh_B is the enthalpy of self-association formation, and Δh_A is the enthalpy of inter-association formation.

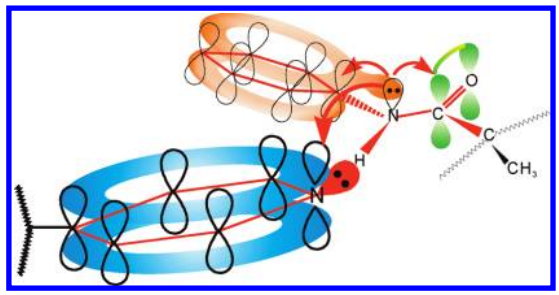

Figure 16. Planar delocalization over carbonyl, phenyl aromatic, and pyridine aromatic π systems via the lone-paired electrons on the nitrogen atom constructed by an inter-associative hydrogen bond between PNPAA and P4VP units.

blend system. In PNMAA/P4VP blends, the value of Δh_A is larger than Δh_B, but immiscible PNMAA/P4VP results are obtained. Similar results are obtained from PNCHAA/P4VP blends. Actually, much larger K_A than K_B does ensure a miscible blend.[1] The K_A/K_B ratios in PNPAA/P4VP blends are higher than those in PNCHAA/P4VP blends at different temperatures. As a result, PNPAA/P4VP blends are miscible over the entire composition range, but PNCHAA/P4VP blends are immiscible on a scale below 20 nm. The much higher K_A/K_B ratios in PNPAA/P4VP blends are a consequence of the planar delocalization. When a pyridine group in P4VP forms a hydrogen bond with the N−H group in PNPAA (see Figure 16), it is suggested that a planar delocalization, constructed by the aromatic-π system of pyridine in P4VP and the aromatic-π system and carbonyl-π system of the amide group in poly(*N*-phenyl methacrylamide)s via the lone-paired electrons on the nitrogen atom of PNPAA, is formed. This planar delocalization is a driving force to replace the self-association of PNPAA with inter-association to P4VP, and thus higher inter-associative equilibrium constants K_B than that in PNMAA/P4VP at different temperatures, even though the phenyl group is more sterically hindered to prevent the formation of any kinds of hydrogen bonding. This planar delocalization is impossible in PNCHAA/P4VP blends, so the steric bulky cyclohexyl group hinders the formation of inter-association and self-association to obtain smaller K_A/K_B at different temperatures.

Conclusions

In this study, poly(*N*-methyl methacrylamide), poly(*N*-cyclohexyl methacrylamide), and poly(*N*-phenyl methacrylamide) are prepared and blended with P4VP, to investigate the resonance effect on self- and inter-associative hydrogen bonding. Through the least-squares curve-fitting procedure and the van't Hoff plots, the enthalpy of self- and inter-associative hydrogen bonding formation can be obtained. All of the results indicate that PNPAA has a smaller enthalpy of self-associative hydrogen bonding formation than that of PNMAA and PNCHAA; however, the enthalpies of inter-associative hydrogen bonding formation of three polymethacrylamides/P4VP blends (PNMAA/P4VP, PNPAA/P4VP, and PNCHAA/P4VP) are comparable. Moreover, the fractions and the equilibrium constants of inter-association under variable temperatures in PNPAA/P4VP are all obviously higher than those in PNCHAA/P4VP blends, indicating that the resonance characteristic of the aromatic ring in PNPAA substantially enhances the ratio $\Delta h_A/\Delta h_B$ to sacrifice its self-association. Thus, PNPAA/P4VP blends are miscible over the entire composition range and PNCHAA/P4VP blends are immiscible from solid-state NMR spectroscopy.

Acknowledgment. This work was supported financially by the National Science Council, Taiwan, Republic of China, under Contract No. NSC 97-2221-E-110-013-MY3 and NSC 97-2120-M-009-003.

References and Notes

(1) Coleman, M. M.; Painter, P. C. *Prog. Polym. Sci.* **1995**, *20*, 1.
(2) Kuo, S. W. *J. Polym. Res.* **2008**, *15*, 459.
(3) Yang, Z.; Han, C. D. *Macromolecules* **2008**, *41*, 2104.
(4) Zhang, X.; Takegoshi, K.; Hikichi, K. *Macromolecules* **1991**, *24*, 5756.
(5) Motzer, H. R.; Painter, P. C.; Coleman, M. M. *Macromolecules* **2001**, *34*, 8390.
(6) Huang, H. L.; Goh, S. H.; Wee, A. T. S. *Polymer* **2002**, *43*, 2861.
(7) Katime, I.; Parada, L. G.; Meaurio, E.; Cesteros, L. C. *Polymer* **2000**, *41*, 1369.
(8) Zhao, J. Q.; Pearce, E. M.; Kwei, T. K. *Macromolecules* **1997**, *30*, 7119.
(9) Chen, W. C.; Kuo, S. W.; Jeng, U. S.; Chang, F. C. *Macromolecules* **2008**, *41*, 1401.
(10) Kuo, S. W.; Chang, F. C. *Macromolecules* **2001**, *34*, 4089.
(11) Kuo, S. W. *Polymer* **2008**, *49*, 4420.
(12) Kuo, S. W.; Liu, W. P.; Chang, F. C. *Macromol. Chem. Phys.* **2005**, *206*, 2307.
(13) Kuo, S. W. *J. Appl. Polym. Sci.* **2009**, *114*, 116.
(14) Kuo, S. W.; Chan, S. C.; Wu, H. D.; Chang, F. C. *Macromolecules* **2005**, *38*, 4729.
(15) Yen, Y. J.; Kuo, S. W.; Huang, C. F.; Chen, J. K.; Chang, F. C. *J. Phys. Chem. B* **2008**, *112*, 10821.
(16) Ouyang, J. Y.; Zhou, S. Q.; Wang, F.; Goh, S. H. *J. Phys. Chem. B* **2004**, *108*, 5937.
(17) Coleman, M. M.; Pehlert, G. J.; Painter, P. C. *Macromolecules* **1996**, *29*, 6820.
(18) Painter, P. C.; Veytsman, B.; Kumer, S.; Shenoy, S.; Graf, J. F.; Xu, Y.; Coleman, M. M. *Macromolecules* **1997**, *30*, 932.
(19) Painter, P. C.; Park, Y.; Coleman, M. *J. Appl. Polym. Sci.* **1998**, *70*, 1273.
(20) Chen, J. K.; Kuo, S. W.; Kao, H. C.; Chang, F. C. *Polymer* **2005**, *46*, 2354.
(21) Kao, H. C.; Kuo, S. W.; Chang, F. C. *J. Polym. Res.* **2003**, *10*, 111.
(22) Kuo, S. W.; Kao, H. C.; Chang, F. C. *Polymer* **2003**, *44*, 6873.
(23) He, Y.; Zhu, B.; Inoue, Y. *Prog. Polym. Sci.* **2004**, *29*, 1021.
(24) Wade, L. G. *Organic Chemistry*; Prentice Hall: NJ, 1987.
(25) Woodford, J. N. *J. Phys. Chem. A* **2007**, *111*, 8519.
(26) Jeffrey, G. A. *An Introduction to Hydrogen Bonding*; Oxford University Press: New York, 1997; Chapter 6.
(27) Liu, S.; Chan, C. M.; Weng, L. T.; Jiang, M. *J. Polym. Sci., Part B: Polym. Phys.* **2005**, *43*, 1924.
(28) Kuo, S. W.; Chang, F. C. *J. Polym. Sci., Part B: Polym. Phys.* **2002**, *40*, 1661.
(29) Zhang, H.; Bhagwagar, D. E.; Graf, J. F.; Painer, P. C.; Coleman, M. M. *Polymer* **1994**, *35*, 5379.
(30) Kuo, S. W.; Lin, C. L.; Chang, F. C. *Macromolecules* **2002**, *35*, 278.
(31) Coleman, M. M.; Painter, P. C. *Miscible Polymer Blends: Background and Guide for Calculations and Design*; DEStech Publications: Lancaster, PA, 2006.
(32) Coleman, M. M.; Graf, J. F.; Painter, P. C. *Specific Interactions and the Miscibility of Polymer Blends*; Technomic Publishing: Lancaster, PA, 1991.
(33) Neelakandan, C.; Kyu, T. *Polymer* **2009**, *50*, 2885.
(34) Coleman, M. M.; Sobkowiak, M.; Pehlert, G. J.; Painter, P. C. *Macromol. Chem. Phys.* **1997**, *198*, 117.
(35) Bhagwagar, Dt.E.; Painter, P. C.; Coleman, M. M.; Krizan, T. D. *J. Polym. Sci., Part B: Polym. Phys.* **1991**, *29*, 1547.
(36) Choperena, A.; Painter, P. *Macromolecules* **2009**, *42*, 6159.
(37) Kamelt, M. J.; Abboud, J. M.; Abraham, M. H.; Taft, R. W. *J. Org. Chem.* **1983**, *48*, 2877.
(38) Zhang, S. H.; Jin, X.; Painter, P. C.; Runt, R. *Polymer* **2005**, *45*, 3933.
(39) Cleveland, C. S.; Fearnley, S. P.; Hu, Y.; Wagman, M. E.; Painter, P. C.; Coleman, M. M. *J. Macromol. Sci., Phys.* **2000**, *B39*, 197.
(40) Tanaka, H.; Nishi, T. *Phys. Rev. B* **1986**, *33*, 32.
(41) Stejskal, E. O.; Schaefer, J.; Sefcik, M. D.; Mckay, R. A. *Macromolecules* **1981**, *14*, 275.
(42) Zhu, B.; Li, J.; He, Y.; Yamane, H.; Kimura, Y.; Nishida, H.; Inoue, Y. *J. Appl. Polym. Sci.* **2004**, *91*, 3565.
(43) Pehlert, G. J.; Painter, P. C.; Coleman, M. M. *Macromolecules* **1998**, *31*, 8423.
(44) Silverstein, R. M.; Bassler, G. C.; Morrill, T. C. *Spectrometric Identification of Organic Compounds*; Wiley: Singapore, 1991; Chapter 3.
(45) Coleman, M. M.; Xu, Y.; Painter, P. C. *Macromolecules* **1994**, *27*, 127.

JP910849Y